Growth of (111)-oriented PZT on RuO_2(100)/Pt(111) electrodes by in-situ sputtering

T. Maeder, P. Muralt, and L. Sagalowicz
Laboratoire de Céramique, Département des Matériaux, Ecole Polytechnique Fédérale de Lausanne, CH-1015 Lausanne, Switzerland

Abstract

Growth of (111)-oriented $Pb(Zr,Ti)O_3$ has been achieved on a RuO_2 film. Necessary condition for the oriented growth was the (100)-orientation of the RuO_2 layer, which could be obtained by using a (111)-textured Pt film as a template. The latter has been grown on thermal oxide of a silicon wafer. XRD and TEM studies have been carried out for finding the orientation relationship between Pt(111), RuO_2(100) and PZT (111).

1 Introduction

During the recent years, the use of ferroelectric thin films of the $PbZr_xTi_{1-x}O_3$ (PZT) family for memory [1], piezoelectric [2] and pyroelectric [3, 4] devices has drawn considerable interest. Reproducible, high quality films require control of the diffusion and nucleation phenomena at the PZT / bottom electrode interface. Platinum is usually used as a bottom electrode, because it has reasonably good thermal stability and is chemically inert in the oxidizing conditions prevailing during PZT processing. Moreover, PZT orientation can be controlled on Pt [5, 6]. However, oxide electrodes such as RuO_2, IrO_2 (rutile structure) and LSCO (perovskite) are superior with respect to fatigue in memory applications [7], and with respect to barrier properties [8, 9] for direct contact geometries. While perovskite electrodes, such as $LaSrCoO_3$ and $SrRuO_3$, are ideal for epitaxial growth of PZT [10], their growth require high temperatures and their chemical stability can be a problem. RuO_2 or IrO_2 are much easier to grow and to integrate. For many applications, an oriented growth of PZT is desirable. However, this is not obvious on rutile structures, and has not been demonstrated yet. Normally the bottom electrode is not grown directly on silicon, but on a buffer layer of thermal oxide, which is an amorphous film. RuO_2 films grown on an adhesion layer (TiO_2) on this amorphous surface do not exhibit preferred orientations [11]. The population of the different orientations can be influenced by growth conditions. However, no well textured films were obtained. Only randomly oriented PZT films have been obtained on such $RuO_2/TiO_2/SiO_2/Si$ substrates. The problem is thus twofold. First, growth of the appropriate orientation of RuO_2 on a suitable template is required. Second, the PZT has to grow oriented on this RuO_2 film.

It is known from the literature that $PbTiO_3$(111) could be obtained on a rutile(100) template [12]. The rutile material was, however, not RuO_2 but SnO_2, and the substrate was not amorphous, but instead was crystalline sapphire. The (100)-oriented SnO_2 was grown onto a sapphire(0001) crystal surface, which exhibits a hexagonal symmetry. In order to follow the same scheme of orientational relations, a hexagonal template for RuO_2 needs to be found first. Good candidates are Pt(111) with a face centered cubic lattice, and Ru(0001) with a hexagonal lattice. Polycrystalline Pt can be grown with (111) texture, even on amorphous substrates [13]. The Pt(111) or Ru(0001) planes have the same topology as the sapphire(0001) planes, and thus the correct epitaxial relationships for RuO_2 (100) are possible. However, the fcc (111) planes can also match with the (110) planes of rutile, as was found by Møller and Wu [14] in the case of Cu films on TiO_2, or also PZT(111) on TiO_2(110) seeding layers [6]. These two possible epitaxial relationships are schematized in Fig. 1, and the in-plane distances and mismatches are given in Table 1.

It is the aim of this paper to show that (111)-oriented PZT can be grown on (100) oriented RuO_2, which could be obtained using a Pt(111) thin film template. First the growth of RuO_2 and SnO_2 on Pt(111) and Ru(0001) thin films are investigated. In a second part the growth of PZT on these electrodes is studied.

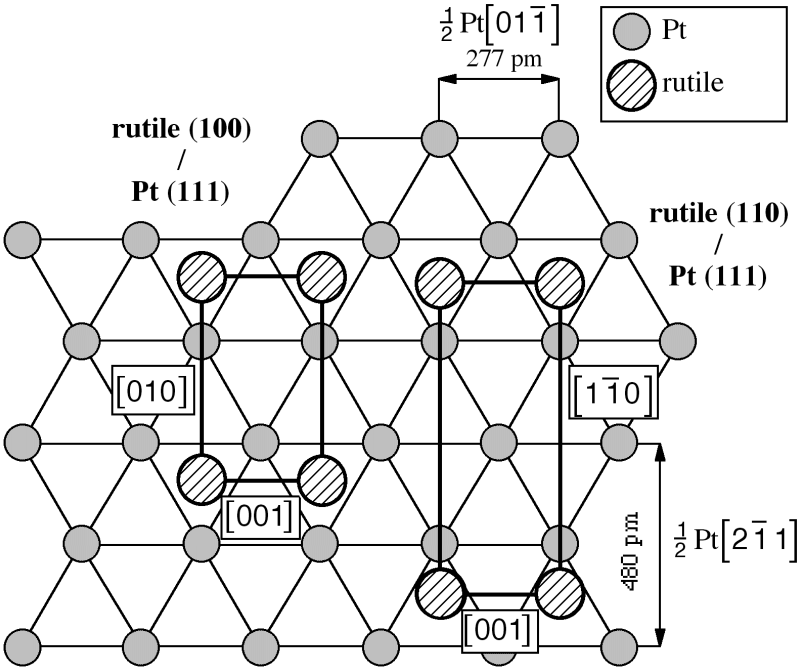

Figure 1. Two probable epitaxial relationships of rutile on a hexagonal surface. The lattice parameters for RuO_2 and Pt have been considered for the drawing. It applies equally well also for the Ru(0001) substrate planes.

	Structure	Plane	Direction 1	Direction 2	d_1 (pm)	d_2 (pm)	Δ_1 (%)	Δ_2 (%)
Pt	fcc	(111)	1/2[01$\bar{1}$]	1/2[2$\bar{1}\bar{1}$]	277	480	0.0	0.0
Ru	hcp	(0001)	1/3[$\bar{1}\bar{1}$20]	[1$\bar{1}$00]	272	471	−2.0	−2.0
RuO_2	rutile	(100)	[001]	[010]	311	450	12.1	−6.3
SnO_2	rutile	(100)	[001]	[010]	319	474	15.0	−1.3
RuO_2	rutile	(110)	[001]	2/3[1$\bar{1}$0]	311	424	12.1	−11.6
SnO_2	rutile	(110)	[001]	2/3[1$\bar{1}$0]	319	447	15.0	−7.0
PT	perovskite	(111)	1/2[01$\bar{1}$]	1/2[2$\bar{1}\bar{1}$]	280	485	1.0	1.0
PZT x = 0.5	perovskite	(111)	1/2[01$\bar{1}$]	1/2[2$\bar{1}\bar{1}$]	288	498	3.8	3.8

Table 1. Calculated in-plane distances and lattice mismatches with Pt(111) for Pt(111), Ru(0001), RuO_2(100) and (110), SnO_2(100) and (110), $PbTiO_3$(111) and PZT(111) at about 550°C (fcc face-centered cubic; hcp hexagonal close packed).

2. Experimental

The film sequences were deposited onto thermally oxidized Si(100) wafers at 400-530 (Pt, Ru), 480 (RuO_2, SnO_2), and 570°C (PZT) by sputtering in a Nordiko 2000 chamber from metal targets (applying reactive mode for the oxides). Process details for the RuO_2 deposition are given in Table 2. It was observed that the film resistivity lowered on increasing the deposition temperature from 50 to 480°C (see Fig. 2). Post-annealing experiments showed that the resistivity of films deposited at a lower temperatures could be decreased, however, the low value of the 480°C film was not reached. In addition, high temperature deposited films are more stable at typical PZT deposition temperatures. For this reason the rather high deposition temperature of 480°C was chosen for this investigation.

For all electrodes, TiO_2 adhesion layers were used [15] on the SiO_2. Well (111)-textured Pt films have been obtained when nucleating the Pt film on the TiO_2 below 400°C. Above this temperature more random orientations were obtained. The Pt(111) thin films served also as templates to obtain well textured Ru(0001) films. $PbZr_xTi_{1-x}O_3$ films were deposited on the RuO_2 by a dynamic in-situ sputtering from three elemental targets [16]. The Ti and Zr magnetrons were operated with dc power, the Pb magnetron with rf power. The films were grown at 570°C with a dynamic rate of 3 nm/min, corresponding to about one unit cell per turn of the substrate carrier. More details of this process are described elsewhere [11,17,18]. Deposition experiments of RuO_2 and SnO_2 on various substrates have been carried out, as listed in Table 3. PZT growth was tested on most of these electrodes. The PZT composition was varied for *x* between 0 and 0.7.

In all cases, PZT deposition was preceded by deposition of a 10 nm thick TiO_2 sacrificial barrier layer to prevent degradation of the RuO_2 surface [11], followed by a nominally 3 nm thick $PbTiO_3$ film allowing better perovskite nucleation [17, 19]. Control of PZT orientation by in-situ sputtering require nucleation with Ti-rich compositions. This is ascribed in most part to their easy nucleation into perovskite. Compared to Pt, RuO_2 necessitates a TiO_2 sacrificial barrier layer in order to prevent destruction of the RuO_2 surface [11]. We believe this to be specific to in-situ reactive magnetron sputtering, specifically of lead, onto RuO_2, due to overoxidation in the plasma. To this date, we have not found any reports of this problem in work involving other deposition methods.

Cathode size of magnetron	100 mm diameter
Dc power	50 W
Sputter gas, 100% O_2	10 mTorr
Substrate temperature	530°C

Table 2. Process parameters of RuO_2 deposition.

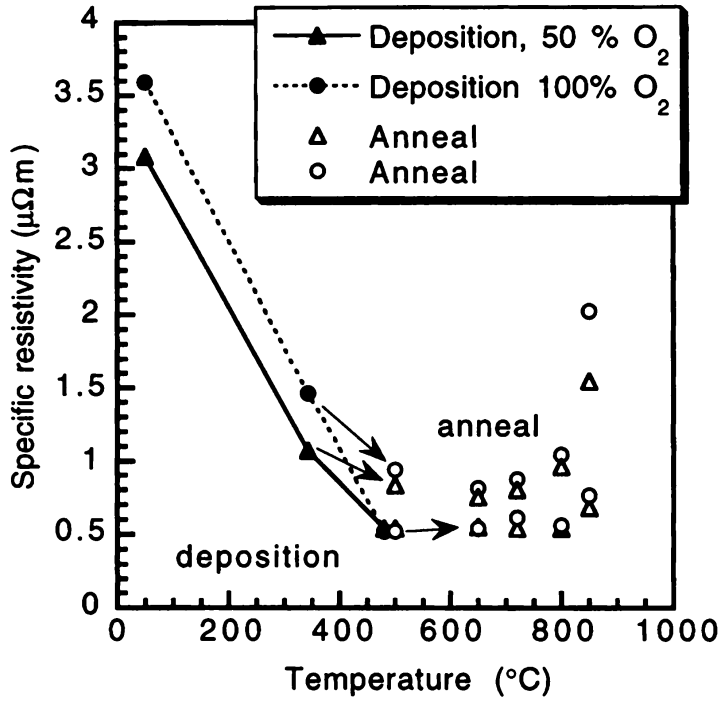

Figure 2. Specific resistivity of RuO_2 films deposited at RT, 340°C and 480°C in pure oxygen and O_2/Ar mixed sputter gas. The films deposited at 340°C and 480°C have been annealed at various temperatures between 500°C and 850°C.

Sample	Material	Substrate
RuO_2/Pt(111)	RuO_2	Pt(111) (on TiO_2/SiO_2/Si)
RuO_2/Ru(0001)	RuO_2	Ru (0001)/Pt(111)/TiO_2/SiO_2/Si
RuO_2/Pt(r)	RuO_2	randomly oriented Pt (on TiO_2/SiO_2/Si)
RuO_2/TiO_2	RuO_2	TiO_2 (on SiO_2/Si)
SnO_2/Pt(111)	SnO_2	Pt(111) (on TiO_2/SiO_2/Si)
SnO_2/TiO_2	SnO_2	TiO_2 (on SiO_2/Si)

Table 3. Sample names of the different variants of layer systems.

3. Results

3.1 X-ray results of RuO_2

Fig. 3 shows XRD spectra of samples RuO_2/Pt(111), RuO_2/Ru(0001) and RuO_2/TiO_2. On TiO_2, all RuO_2 peaks are present, and only a slight (100) texture is obtained. On the other hand, films on oriented Pt and Ru show a strong (100)-orientation. On Pt (111), no RuO_2 peak is found except for the Pt(111) peak, which coincides with the one of RuO_2(200). As the RuO_2 had normal aspect and thickness, we can infer it is (100) oriented.

On Ru(0001)/Pt(111) the eventual RuO_2(100) peak is again hidden in the Pt(111) peak. Besides the Ru(0001) reflection, two reflections from RuO_2, (110) and (220) can be seen. Therefore, the film can be (110) or mixed (110) + (100) oriented. When Ru was grown directly onto Ti/SiO_2 (Ti adhesion layer), the Ru was also (0001) oriented, albeit with a very slight ($1\underline{1}01$) contribution. On this film, RuO_2 (110) and (200) contributions, together with their higher orders, are clearly visible. No other oriention are observed. It is thus logic to assume that also the film grown on Ru(0001)/Pt(111) exhibits mixed (110) and (100) orientation.

The direct growth on the TiO_2 adhesion layer lead to a weakly textured film. Although (200) is by far the largest peak, the low reflection intensity indicates that there is a bad alignment between substrate and the low-index planes of a large fraction of grains.

Since RuO_2(200) and Pt(111) XRD peaks cannot be resolved, complementary tests were necessary to confirm the results. This problem was solved by taking a rocking curve scan of the RuO_2(310) peak, whose plane has a small angle (18.4°) to the (100) RuO_2 plane (and Pt(111) plane). If, as we tentatively concluded, the (100) planes of RuO_2 lie parallel to the substrate, the (310) planes will make a 18.4° angle with the latter, and the (310) rocking curve must have 2 peaks near $\alpha = \pm 18.4°$. The rocking curves, with different corrections, are shown in Fig. 4. The broad $\alpha = 0$ peak is due to the proximity of the extremely intense Si(400) peak.

If we suppose random orientation in the plane, the curve must be weighed with a $|\sin \alpha|$ factor. The result is given in the second part of Fig. 4. Two peaks are indeed observed at $\alpha \sim \pm 18°$ (dashed lines), in excellent agreement with the 18.4° value, proving the RuO_2 is indeed (100) oriented. Moreover, the width of the peaks (±3°, dotted lines in left peak) is similar to that of the Pt itself, indicating that only a small degradation of the orientation takes place. These rocking curve results prove that practically all (310) planes of the film belong to (100)-oriented grains. Since no other phases or amorphous parts have been detected by θ-2θ scans, a strong (100)-texture of the RuO_2 film can be assumed.

If the (100) orientation is the result of epitaxy on (111)-oriented Pt grains, growth on randomly oriented platinum should not exhibit a preferred orientation. This test was performed in another series of coatings. Figure 5 shows XRD spectra of samples RuO_2/Pt(111), RuO_2/Pt(r) and RuO_2/TiO_2, using thicker (300 nm) RuO_2 films. While the (100) orientation is maintained on Pt(111), all RuO_2 peaks are visible on the more random Pt. Good (111) orientation of the Pt is

therefore a prerequisite for (100)-RuO_2, showing that the relationship is indeed epitaxial in origin.

Finally it was also checked whether the same epitaxial orientation relationship between RuO_2 and Pt(111) does also hold for SnO_2. The XRD spectra of a coating series are shown in figure 6. The results are similar, as it can clearly be seen that the SnO_2 film (SnO_2/Pt(111)) orients well on Pt(111), much better than on TiO_2 (SnO_2/TiO_2), amplified by factor 20 in Fig. 6. However, the orientation is bimodal, i.e. both (110) and (200) peaks are visible. The (100) orientation is dominant, though. It is not excluded that with an adjustment of the deposition process, an improvement of texture could be obtained.

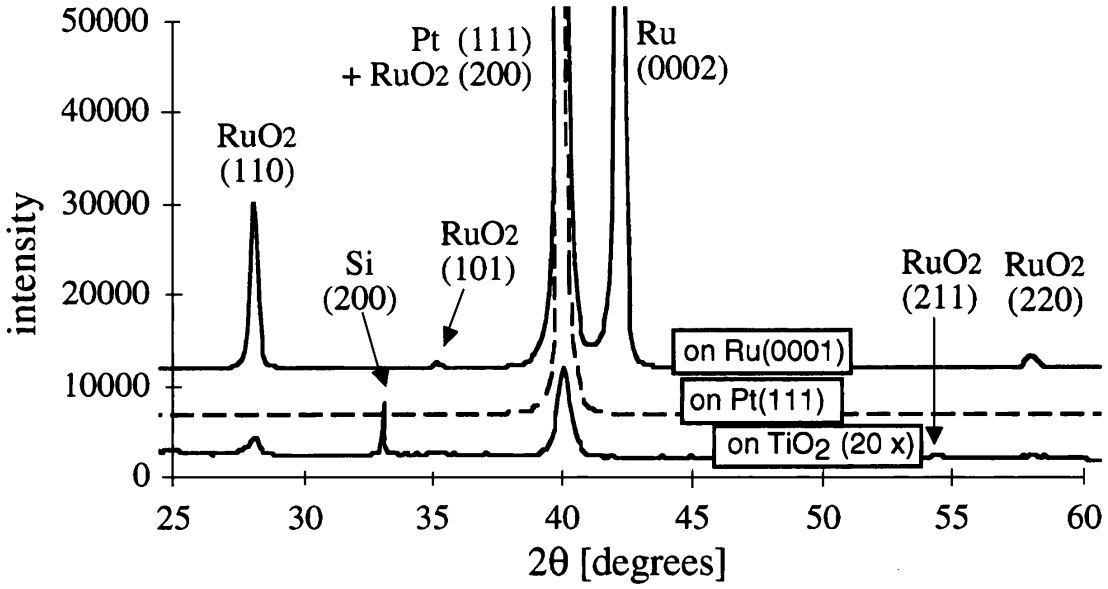

Figure 3. XRD (θ-2θ) spectra of 100 nm RuO_2 films on Pt(111), Ru(0001) and TiO_2.

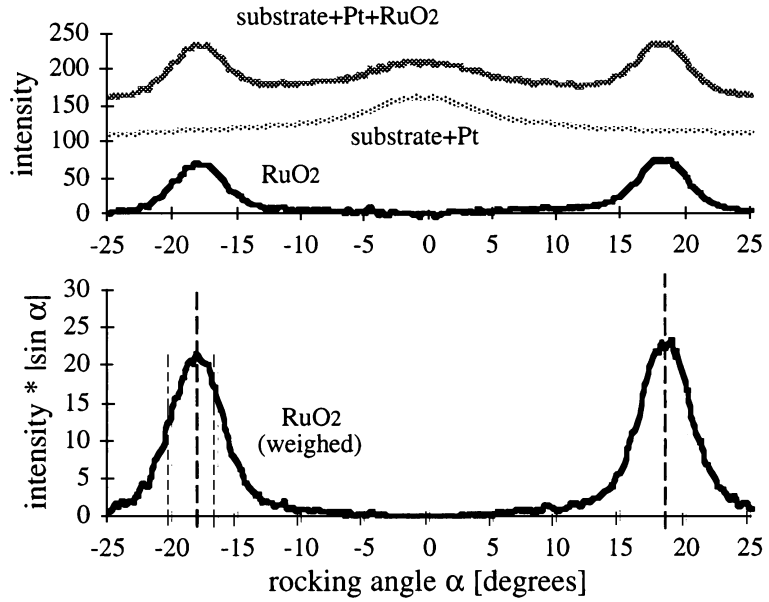

Figure 4. XRD rocking curve of the RuO_2(310) peak of a film grown on Pt(111) (sample RuO_2/Pt(111)).

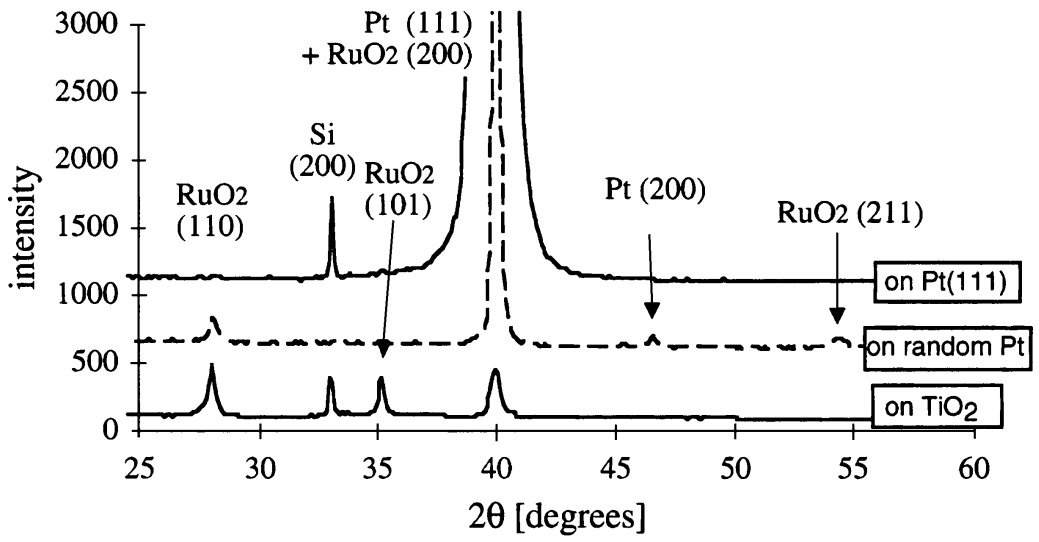

Figure 5. XRD (θ-2θ) spectra of RuO_2 on Pt(111), Pt 'random' and TiO_2.

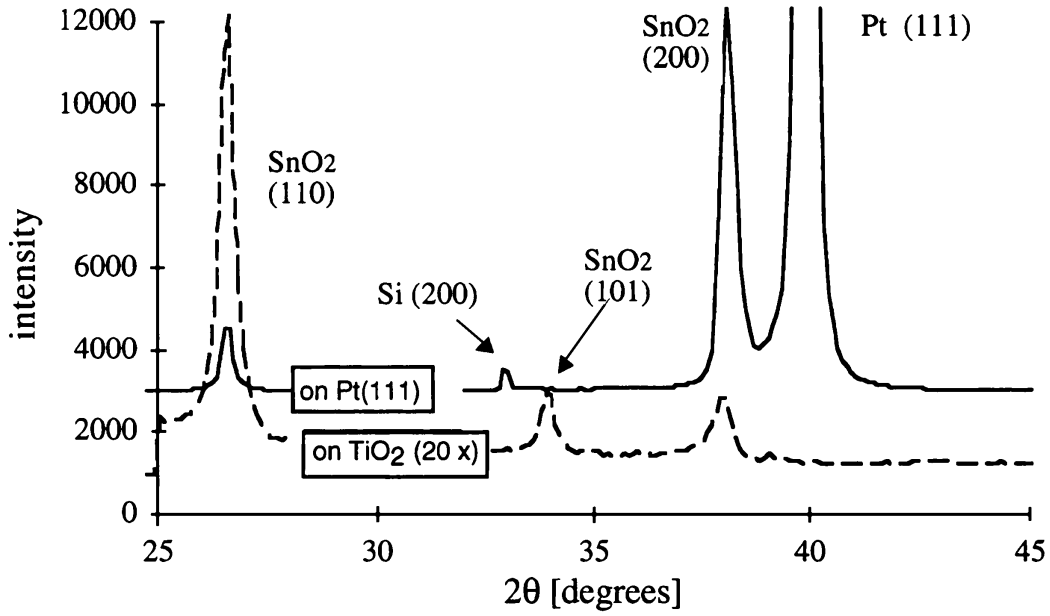

Figure 6. XRD (θ-2θ) spectra of 100 nm SnO_2 films on Pt(111) and TiO_2.

3.2. X-ray results of PZT on RuO_2

Fig. 7 shows the XRD spectra of a 300 nm thick PZT film ($x = 0.45$) deposited on (100) and "randomly" oriented RuO_2 (RuO_2/Pt(111) and RuO_2/TiO_2 resp.). While the orientation of the PZT is essentially random on the "random" RuO_2, a strong (111) orientation develops on the (100) - oriented RuO_2, again demonstrating the existence of an orientation relationship and extending the results of Chang et al. [12] on $PbTiO_3$ / SnO_2 to a similar system, namely PZT / RuO_2. This result has been confirmed for a wide range of x values, as is shown in Fig. 8. Strong (111) orientation is found for all compositions on (100) RuO_2, especially towards high values of x. Conversely, all PZT films were essentially randomly oriented on "random" RuO_2.

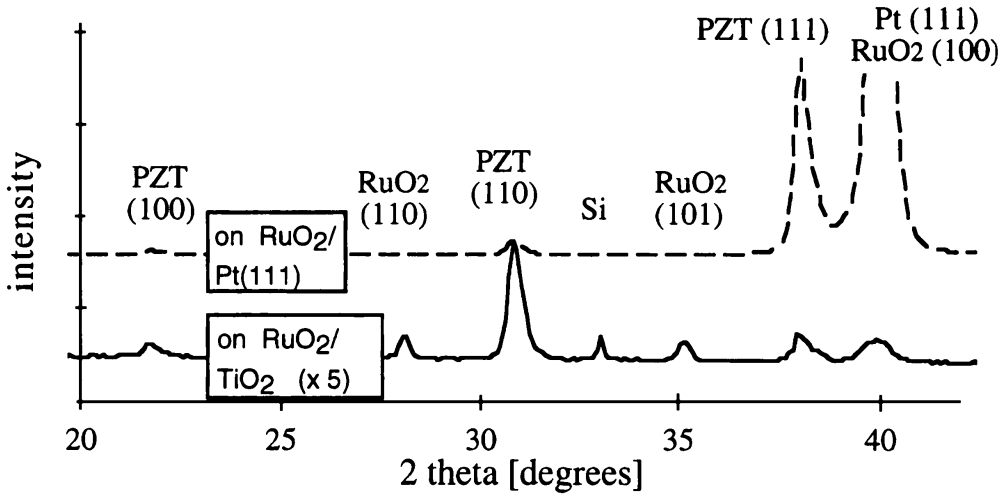

Figure 7. XRD (θ-2θ) spectra of PZT (x = 0.45) films, deposited on (100)-oriented and 'random' RuO_2.

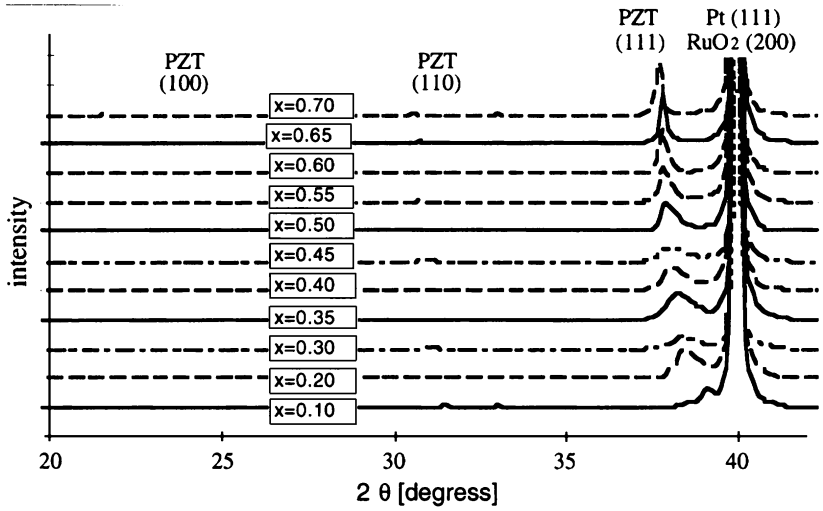

Figure 8. XRD (θ-2θ) spectra of $PbZr_xTi_{1-x}O_3$ films on (100)-oriented RuO_2/ Pt(111), with x ranging from 0.1 to 0.7.

3.3 Transmission Electron Microscopy observations

Cross section TEM images were obtained for the PZT thin film deposited onto 100 nm RuO_2/Pt(111). Fig. 9 shows a dark field image of the different layers. No sign of second phase at the interface between the Pt and the RuO_2 is present. In particular the 10 nm TiO_2 layer between the RuO_2 and the PZT seems to have dissolved in the PZT or in the RuO_2. This result was confirmed by high resolution images (HRTEM) [20]. The sacrificial layer of TiO_2 most likely dissolves in the PZT as it is the case for PZT deposited onto Pt when a thin TiO_2 seed layer is used [6]. Some defects at the interface TiO_2-Pt are observed and they probably result from limited diffusion between the TiO_2 and the Pt layers but no sign of Pb was found in the TiO_2 or in the SiO_2 using energy dispersive spectrometry which show that the composite electrode (RuO_2/Pt) is a very good diffusion barrier.

Fig. 10 shows a HRTEM image of the Pt-RuO_2 interface. For this image, the orientation was determined. In the Pt, lines parallel to the interfaces are visible. Those are separated by about 0.22 nm. This is in agreement with the distance between the (111) plane of Pt (0.2265 nm). This

demonstrates that this platinum grain has the (111) orientation. The RuO_2 shows a square arrangement which corresponds to distance of 0.31 nm which is close to (110) distance of the RuO_2 (0.3183 nm). Therefore the beam was parallel to [001] RuO_2 and as indicated in Fig.9, the [200] RuO_2 direction is normal to the interfaces. Therefore the orientation of the RuO_2 is (100) which confirms the X-ray results.

In order to understand the difference in orientation when the RuO_2 is deposited directly onto TiO_2 (without a Pt template), the interface between TiO_2 and RuO_2 was also studied (Fig. 11). First no intermediate layer is observed and the interface appears relatively sharp. Therefore interdiffusion is probably limited. Secondly, there is no change between the orientation in the TiO_2 and in the RuO_2. Therefore, the RuO_2 has grown cube on cube onto TiO_2. This is logical since the RuO_2 and the TiO_2 both have the rutile structure and the lattice mismatch is relatively small (about 2% for the axis and about 5% for the c axis).

Figure 9. TEM dark field image of the layer sequence PZT/RuO_2/Pt/TiO_2/ thermal oxide.

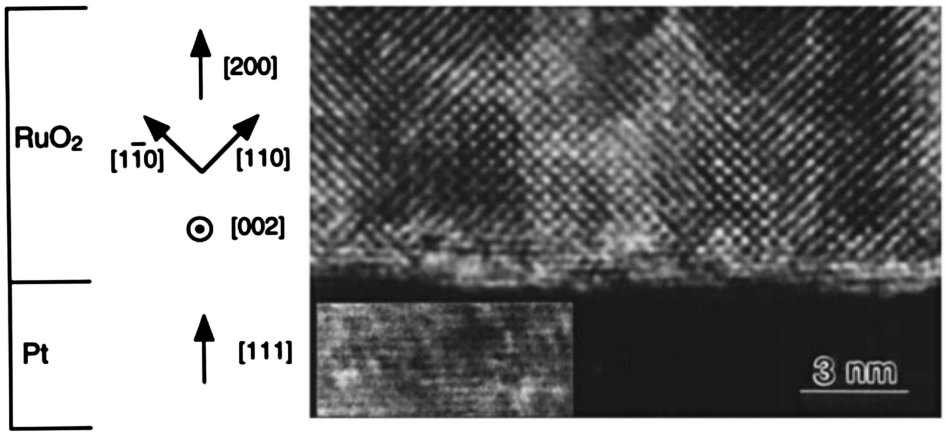

Figure 10. HRTEM image showing the orientational relation between RuO_2(100) planes and Pt(111) planes. The inset was taken in the same platinum grain but at a location where the Pt lattice fringes were visible.

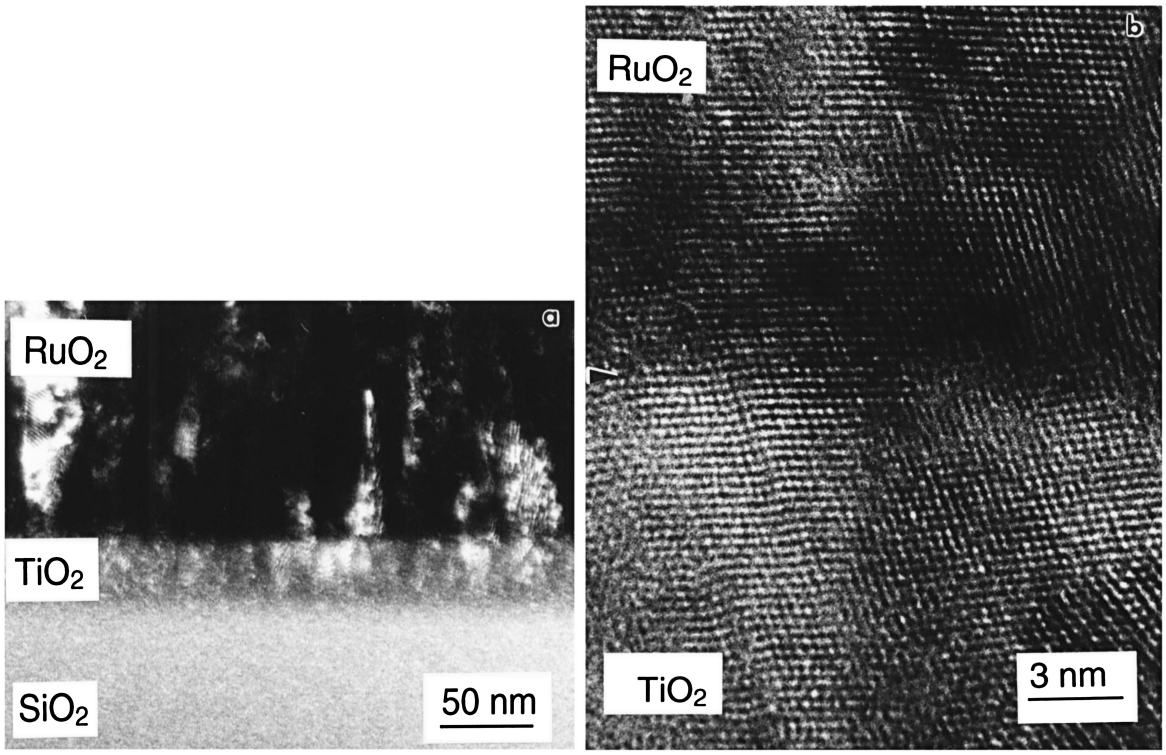

Figure 11. TEM images of the RuO_2-TiO_2 interface: (a) dark feld image, (b) HRTEM image, showing the 'cube on cube' orientation relationship between RuO_2 and TiO_2. The interface is marked by an arrow.

4. Discussions

The orientation of RuO_2 and SnO_2 films is very much influenced by the substrate on which nucleation takes place. Our results show that both orientations of rutile - (100) and (110) - can grow on the hexagonal planes of close-packed (111) planes of the Pt face-centered cubic (fcc) lattice and (0001) planes of the Ru hexagonal (hcp) lattice. In other systems similar results have been obtained. Chang et al. [12] grew (100) epitaxial SnO_2 on Al_2O_3 (0001) crystals, which have the same topology as Pt(111) and Ru(0001). Møller and Wu [14] showed that a thin Cu film grows (111) on (110) rutile TiO_2, and has an epitaxial relationship in one of the in-plane directions. In another work, it was shown that nanometer thick films of TiO_2 grow in (110) orientation on Pt(111) [6]. In the case of deposition of the RuO_2 directly onto TiO_2, we have found the orientation was random with perhaps a small preferred (100)-orientation.

The orientation of the nuclei depends on both surface and interface energy. This investigation indicates that the interface is more important than the surface, since the orientation depends on the substrate. It might be that the surface energy helps to promote the observed orientations (110) and (100), since they happen to be the ones with the lowest surface energies of rutile TiO_2 [21]. RuO_2 (100) exhibits clearly the lowest interface energy with the close-packed planes, despite the relatively large misfit of around 10 % (see table 1). With the certainly small thickness of the nuclei the lattice can easily deform. During growth, defects such as dislocations relax the stress while keeping the same orientation. In case of SnO_2, it must be assumed that both orientations exhibit to a similar overall energy.

In the case of growth onto TiO_2, there is mainly a cube on cube orientation relationhip between neighboring grains of the two rutiles, and therefore the orientation of the TiO_2 layer determines also the orientation of the RuO_2. Since the first one grows randomly oriented on the amorphous thermal oxide, the resulting orientation of RuO_2 is also random.

TEM observation of the PZT/RuO_2 interface show no traces of the interfacial TiO_2 layer after PZT growth. This can happen either by dissolution into RuO_2 or conversion to $PbTiO_3$. The second

possibility appears to be more likely, as the TiO_2 adhesion layer below RuO_2 shows little interdiffusion with RuO_2, if any. There remains the question whether perovskite nucleation takes place on the thin layer of TiO_2 or on the RuO_2 after diffusion of lead through this thin titania (TiO_2) layer. Since titania is a very good seed for $PbTiO_3$ nucleation [6], both may happen. The thin titania layer may grow with the identical orientation as RuO_2, as is the case of the reversed order. This work clearly shows orientation relationships along the whole PZT(111) / RuO_2(100) / Pt(111) trilayer structure. PZT(111) can also be grown directly on Pt(111) by means of TiO_2 seeding [6]. Therefore, the method presented in this paper will contribute to compare PZT films on RuO_2 and Pt having the same (111) orientation.

Conclusions

We have shown (111) oriented PZT films can be grown much the same way as on Pt(111), by inserting a RuO_2(100) film, allowing comparison on the two electrodes of films having the same crystalline orientation. The textured growth of RuO_2 was achieved on a platinum (111) film, in analogy to SnO_2/sapphire where the hexagonal planes of the sapphire crystal serve as template [12]. In our case, no crystal plane was needed. The substrate was an amorphous thermal oxide layer. It is thus possible to grow PZT(111) films on RuO_2, using passivated silicon wafers (as schematically presented in fig. 12). Extension of the work to RuO_2 on Ru(0001) and SnO_2 on Pt(111) show that both the (110) and the (100) oriented rutile grows on the dense planes of the fcc and hcp lattices. For reasons of surface energy, lattice parameters or deposition conditions, RuO_2(100) has been obtained almost exclusively on Pt(111).

Acknowledgments

The authors would like to thank Dr. Pedro Möckli for his help in X-ray diffraction and Prof. Nava Setter for continuous support. The TEM work was performed at the CIME - EPFL. This work was funded by the Swiss Priority Program for Materials.

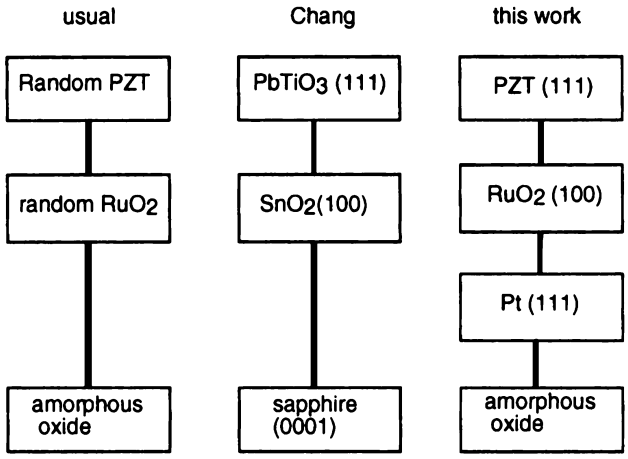

Figure 12. Schematic presentation of the layer sequences usually used for random PZT on RuO_2 electrodes, and the oriented solution achieved in this work. The hexagonal plane - rutile sequence as obtained with sapphire substrates (see ref. [12]) could be realized by textured Pt(111) films.

References

1. R.E. Jones Jr., P. Zurcher, P. Chu, D.J. Taylor, Y.T. Lii, B. Jiang, P.D. Maniar, S.J. Gillespie, "Memory applications based on ferroelectric and high-permittivity dielectric thin films", *Microelectronic Engineering* **29** (1995) 3-10.
2. P. Muralt, M. Kohli, T. Maeder, A. Kholkin, K.G. Brooks, N. Setter, R. Luthier, "Fabrication and characterization of PZT thin film vibrators for micromotors", *Sensors and Actuators A* **48** (1995) 157-165.
3. R. Takayama, Y. Tomita, K. Iijima, and I. Ueda,"Pyroelectric properties and application to infrared sensors of $PbTiO_3$, $PbLaTiO_3$ and $PbZrTiO_3$ ferroelectric thin films", *Ferroelectrics* **118** (1991) 325-342.
4. M. Kohli, Y. Huang, T. Maeder, C. Wuethrich, A. Bell, P. Muralt, N. Setter, P. Ryser, M. Forster,"Processing and properties of thin film pyroelectric devices", *Microelectronic Engineering* **29** (1995) 93-96.
5. P. Muralt, T. Maeder, S. Scalese, D. Naumović, R.G. Agostino, N. Xanthopoulos, H.-J. Mathieu, "In-situ sputter deposition of $PbTiO_3$ thin films: nucleation on textured platinum films", *5th Int. Symp. on Trends and New Applications in Thin Films, Colmar, 1996, Le Vide: science, technique et application* **279** (1996) 45.
6. P. Muralt, T. Maeder, L. Sagalowicz, S. Scalese, D. Naumović, R.G. Agostino, N. Xanthopoulos, H.-J. Mathieu, L. Pathey, E.L. Bollock, "Texture control of $PbTiO_3$ and $Pb(Zr,Ti)O_3$ thin films with TiO_2 seeding", *Journal of Applied Physics* **83** (1998) 3835-3841.
7. R. Ramesh, H. Gilchrist, T. Sands, V. G. Keramidas, R. Haakenaasen, D. K. Fork, "Ferroelectric La-Sr-Co-O/Pb-Zr-Ti-O/La-Sr-Co-O heterostructures on silicon via template growth", *Applied Physics Letters* **63** (1993) 3592-94.
8. T. Maeder, P. Muralt, L. Sagalowicz, I. Reaney, M. Kohli, A. Kholkin, N. Setter, "$Pb(Zr,Ti)O_3$ thin films on zirconium membranes for micromechanical applications", *Applied Physics Letters* **68** (1996) 776-778.
9. T. Maeder, P. Muralt, L. Sagalowicz, and N. Setter, "Conducting barrier electrodes for direct contact of PZT thin films on tungsten", *Journal of the Korean Physical Society* **32** (1998) S1569.
10. R. Ramesh, A. Inam, B. Wilkens, W. K. Chan, T. Sands, J. M. Tarascon, D. K. Fork, T. H. Geballe, J. Evans, and J. Bullington, "Ferroelectric bismuth titanate/superconductor (Y□Ba□Cu□O) thin□film heterostructures on silicon", *Applied Physics Letters* **9** (1991) 1782-1784.
11. T. Maeder, P. Muralt, L. Sagalowicz, and N. Setter, "In-situ sputter deposition of PT and PZT films on platinum and RuO_2 electrodes", *Microelectronic Engineering* **29** (1995) 177-180.
12. H.L.M. Chang, H. Zhang, Z. Shen, and Q. Wang, "Epitaxial thin films of $PbTiO_3$ / SnO_2 heterostructures on sapphire", *Journal of Materials Research* **9** (1994) 3108-3112.
13. K.G. Brooks, I.M. Reaney, R. Klissurska, Y. Huang, L. Bursill and N. Setter, "Orientation of rapid thermally annealed lead zirconate titanate thin films on (111) Pt substrates", *Journal of Materials Research* **9** (1994) 2450-2553.
14. P.J. Møller and M.-C. Wu, "Surface geometrical structure and incommensurate growth: Ultrathin Cu films on TiO_2(110)", *Surface Science* **224** (1989) 265-276.
15. K. Sreenivas, I. Reaney, T. Maeder, N. Setter, C. Jagadish, R.G. Elliman, "Investigation of Pt/Ti bilayer metallization on silicon for ferroelectric thin film integration", *Journal of Applied Physics* **75** (1994) 232-239.
16. R. Bruchhaus, H. Huber, D. Pitzer, and W. Wersing, "Deposition of ferroelectric PZT thin films by planar multi-target sputtering", *Ferroelectrics* **127** (1992) 137-142.
17. T. Maeder, P. Muralt, M. Kohli, A. Kholkin, and N. Setter, "$Pb(Zr,Ti)O_3$ thin films by in-situ reactive sputtering on micromachined membranes for micromechanical applications", *British Ceramic Proceedings* **54** (1995) 207-218.
18. T. Maeder and P. Muralt, "In-situ thin film growth of $PbTiO_3$ by multi target sputtering", *Materials Research Society Symposium Proceedings* **341** (1994) 361-366.
19. O. Auciello, K.D. Gifford, and A.I. Kingon, "Control of structure and electrical properties of lead-zirconium-titanate-based ferroelectric capacitors produced using a layer-by-layer ion-beam sputter-deposition technique", *Applied Physics Letters* **64** (1994) 2873-2875.
20. T. Maeder, P. Muralt, L. Sagalowicz, I. Reaney, M. Kohli, A. Kholkin, N. Setter, "$Pb(Zr,Ti)O_3$ thin films on zirconium membranes for micromechanical applications", *Applied Physics Letters* **68** (1996) 776-778.
21. J. Ziółkowski, "New method of calculation of the surface enthalpy of solids", *Surface Science* **209** (1989) 536-561.